In vitro and *in vivo* biocompatibility studies of a recombinant analogue of spidroin 1 scaffolds

M. M. Moisenovich,[1] O. L. Pustovalova,[1] A. Yu Arhipova,[1] T. V. Vasiljeva,[1] O. S. Sokolova,[1] V. G. Bogush,[2] V. G. Debabov,[2] V. I. Sevastianov,[3] M. P. Kirpichnikov,[1] I. I. Agapov[3]

[1]Faculty of Biology, Lomonosov Moscow State University, Leninskiye Gory 1, Building 12, 119991 Moscow, Russian Federation
[2]Laboratory for Protein Engineering, The State Scientific Center of Russian Federation "The State Research Institute for Genetics and Selection of Industrial Microorganisms," 1st Dorozhny 1, 117545 Moscow, Russian Federation
[3]Research Center for Biomaterials, Shumakov Federal Research Center of Transplantology and Artificial Organs, Shchukinskaya 1, 123182 Moscow, Russian Federation

Received 25 August 2010; accepted 1 September 2010
Published online 4 November 2010 in Wiley Online Library (wileyonlinelibrary.com). DOI: 10.1002/jbm.a.32968

Abstract: The goal of this study was to generate porous scaffolds from the genetically engineered protein, an analogue of *Nephila clavipes* spidroin 1 (rS1/9) and to assess the properties of new rS1/9 scaffolds essential for bioengineering. The salt leaching technique was used to make the rS1/9 scaffolds of interconnected macroporous structure with spontaneously formed micropores. The tensile strength of scaffolds was 18 $\pm$ 5 N/cm^2. Scaffolds were relatively stable in a phosphate buffer but degraded in oxidizing environment after 11 weeks of incubation. Applicability of the recombinant spidroin 1 as a substrate for cell culture was demonstrated by successful 3T3 cells growth on the surface of rS1/9 films (270 $\pm$ 20 cells/mm^2 *vs.* 97 $\pm$ 8 cells/mm^2 on the glass surface, $p < 0.01$). The 3T3 fibroblasts readily proliferated within the rS1/9 scaffold (from initially plated 19 $\pm$ 2 cells/mm^3 to 3800 $\pm$ 304 cells/mm^3 after 2 weeks). By this time, cells were uniformly distributed between the surface and deeper layers (27% $\pm$ 8% and 33% $\pm$ 4%, respectively; $p > 0.05$), whereas the initial distribution was 58% $\pm$ 7% and 11% $\pm$ 8%, respectively; $p < 0.05$). The rS1/9 scaffolds implanted subcutaneously into Balb/c mice were well tolerated. Over a 2-month period, the scaffolds promoted an ingrowth of *de novo* formed vascularized connective tissue elements and nerve fibers. Thus, scaffolds made of the novel recombinant spidroin 1 analogue are potentially applicable in tissue engineering. © 2010 Wiley Periodicals, Inc. J Biomed Mater Res Part A: 96A: 125–131, 2011.

Key Words: spidroin, biopolymer, biodegradable scaffold, biocompatibility

INTRODUCTION

New biomaterials as scaffolds for artificial tissues and organs are extensively investigated. Biocompatible and biodegradable scaffolds can support cell attachment and proliferation, as well as three-dimensional (3D) orientation of tissues.[1–3] Natural silk derivatives have been widely used for these purposes. The most popular source of silk is the cocoon of the silkworm *Bombix mori*.[4] Recently, many other types of silk have attracted the attention of research groups worldwide.[5–8] The spider dragline silk of *Nephila clavipes* consists of two fibrillar proteins (spidroins 1 and 2).[9] Because the biomedical applications of natural spider silk are limited because of insufficient amount of material, the recombinant analogues of spidroins have been recently developed.[10,11] The genetically engineered protein, an analogue of *N. clavipes* spidroin 1 (rS1/9), possesses all typical properties of full-length spidroins, that is, the ability for structural transition to the beta-sheet structure, a spontaneous formation of nanofibrils and microspheres in aqueous solutions, and the formation of tough fibers after spinning.[12,13]

The goal of this study was to prepare the scaffolds based on recombinant spidroin 1 and to investigate their structural and mechanical properties. It was shown that recombinant spidroin 1 scaffolds are suitable for eukaryotic cell culture as well as for *in vivo* evaluation of the tissue response to implants.

MATERIALS AND METHODS

Purification of recombinant protein

The artificial gene S1/9 consists of nine chemically synthesized "monomers" 1f1.[12] They were amplified as part of the plasmid followed by transformation into yeast cells of *Pichia pastoris*. The expressed rS1/9 protein was purified from yeast cell extract by the method developed previously,[12]

Correspondence to: M. M. Moisenovich; e-mail: mmoisenovich@mail.ru
Contract grant sponsor: Russian Foundation for Basic Research; contract grant number: 09-02-00173-a
Contract grant sponsor: Federal Program "Research and Education Staff for Innovative Russia, 2009–2013" of the Ministry of Education and Science of Russian Federation; contract grant numbers: P2460, P2087, P816, P407

including acidification, heating, ultrafiltration, and chromatography on a weak cation exchanger SP Sepharose Fast Flow (Amersham Biosciences, Uppsala, Sweden) in a fast protein liquid chromatography system by a two-step pH-gradient elution. A high purity of the sample was confirmed using sodium dodecyl sulfate-polyacrylamide gel electrophoresis and spectrophotometry.

Preparation of the rS1/9 films and scaffolds

The lyophilized biopolymer rS1/9 was dissolved in 10% lithium chloride in 90% formic acid. The samples were agitated for 40 min to facilitate dissolution, and then the solutions were centrifuged for 10 min at 11,300*g*. The rS1/9 films were formed using the casting method.[10] A drop of diluted (1 mg/mL) biopolymer solution was applied to the surface of a smooth carrier for 1 h at room temperature. After drying, the films (diameter 2 cm and thickness 80 mm) were immersed in 96% ethanol.

The porous scaffolds were prepared from biopolymer rS1/9 solutions (300 mg/mL) using the salt leaching technique. Particles of dry granular (200–400 μm) NaCl were added to the biopolymer solution (110 mg of salt per 50 μL). Two types of containers for scaffold formation were used: disk-shaped containers (10 mm in diameter, approximately 1 mm deep) and bar-shaped ones (width 3 mm, approximate length 12 mm). Shaped scaffold samples were dried at room temperature, then treated in 96% ethanol, and immersed in distilled water to remove NaCl. The samples were degassed using a vacuum pump for 1 h and sterilized by soaking in 96% ethanol for 2 h. During this procedure, rS1/9 adopts the beta-sheet structure.[14]

Characterization of the rS1/9 scaffolds

The structure of the rS1/9 scaffolds was analyzed with a scanning electron microscope. The scaffold samples were prepared according to standard procedure and sputter-coated with 20-nm-thick gold. The specimens were examined using a Camscan S2 (Cambridge Instruments, Cambridge, UK) in SEI mode with a 10-nm optical resolution and an operating voltage of 20 kV. The images were captured using MicroCapture software (SMA, Russian Federation).

The structure of the rS1/9 scaffolds in aqueous environment was analyzed using a confocal laser scanning microscope Axiovert 200M LSM510 META (Carl Zeiss, Jena, Germany) equipped with Plan-Neofluar 10×/0.3, Plan-Neofluar 20×/0.5, and Plan-Neofluar 40×/1.3 objectives. For confocal laser scanning microscopy (CLSM), the rS1/9 scaffold was treated with tetramethyl rhodamine isothiocyanate (Sigma). To prepare the staining solution, tetramethyl rhodamine iso-thiocyanate was dissolved in dimethylsulfoxide (1 mg in 20 μL) and the resulting solution was diluted 20 times with 0.1*M* bicarbonate buffer, pH 9.6. The scaffolds were incubated in the staining solution for 12 h. To terminate conjugation, the samples were immersed in a 0.1*M* Tris-HCl buffer, pH 7.6, for 30 min followed by rinsing with phosphate-buffered saline (PBS).

To investigate the rS1/9 scaffold degradation *in vitro*, the samples of scaffold were incubated in PBS or Fenton's reagent (0.1 m*M* $FeSO_4$, 1 m*M* H_2O_2). The rate of the rS1/9 scaffold degradation was assessed by weekly measurement of weight of the scaffold samples for up to 14 weeks.

To measure the tensile strength and extensibility of the porous scaffolds, one end of the dry bar-shaped sample was fixed in a clip and the other was loaded with a known weight. The weight was increased until the sample ruptured. The tensile strength (N/cm^2) was calculated as the ratio of the rupture weight per cm^2 of the cross-section area of the sample. The extensibility of the sample was calculated as the ratio of the original length to the length after elongation.

Cell growth and cell adhesion assays

The rS1/9 scaffolds and films were used for culturing 3T3 fibroblasts. The scaffolds or films were placed into 24-well plates. The 3T3 murine fibroblast cells (24,000 cells/mL) were plated in 300 μL of Dulbecco's modified Eagle's medium supplemented with 10% fetal bovine serum (Sigma). After the cells adhered to the substrate (40 min for films and 2 h for scaffolds), the samples were rinsed to remove unattached cells. The fibroblasts attached to the rS1/9 scaffold were incubated for up to 2 weeks. The culture medium was changed every 2 days. Cell attachment and proliferation were studied using scanning electron microscopy (SEM) and CLSM. After the completion of cell culture, the scaffolds were fixed for 30 min in 4% paraformaldehyde and treated for 10 min with 0.1% Triton X-100 in PBS. Cell nuclei were stained with SYTOX® Green (Invitrogen, Carlsbad, CA) and counted in CLSM images. An area of 4.2 mm^2 of each thin film and a volume of 2.55 mm^3 of each 3D scaffold were examined. The depth of scaffold samples was studied up to 600 μm. The calculations were performed using 3D for LSM Version 1.4.2 (Carl Zeiss) and Imaris 6.1.5 (Bitplane AG, Zurich, Switzerland).

Implantation of the rS1/9 scaffolds

Five 12-week-old locally bred female BALB/c mice were used for implantation. All procedures of animal keeping and handling were performed according to the protocols approved by the Animal Care and Use Committee, in compliance with the guidance of the Ministry of Health Care and Social Development of the Russian Federation, document no. 755 issued on December 8, 1977, and the World Medical Association's Declaration of Helsinki (2000). During surgical procedures, mice were anesthetized by Zoletil 100 injected intraperitoneally (Virbac Laboratories, Carros, France) (5 mg/100 g). The bar-shaped rS1/9 scaffolds were aseptically implanted into midline dorsal subcutaneous areas.

Histology

The samples were harvested 8 weeks after surgery and fixed in Bouin's fixative solution. Samples were dehydrated in a series of alcohols, embedded in Histomix® (BioVitrum, Russian Federation) and cut into 5-μm slices. Sections were

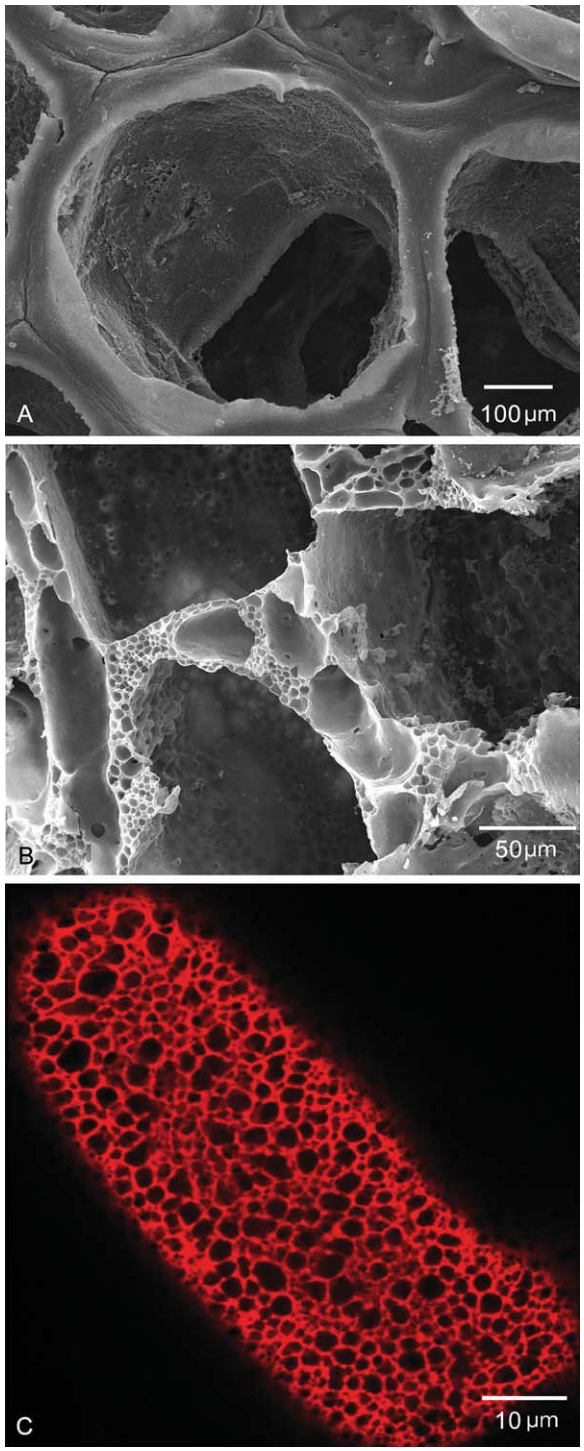

FIGURE 1. Structure of the rS1/9 scaffolds. (A) SEM image of interconnected, porogen-generated macroporous structure. (B) SEM image of spontaneously formed sponge-like microporous structure of the walls of macropores. (C) CLSM image of optical cross-section of the scaffold shows microporous structure preserved in aqueous environment. The scaffolds were conjugated with tetramethyl rhodamine isothiocyanate. [Color figure can be viewed in the online issue, which is available at wileyonlinelibrary.com.]

deparaffinized, rehydrated, stained with hematoxylin and eosin, and visualized with a Zeiss Imager A1 (Zeiss) and a high-resolution camera AxioCam MRc 5 (Zeiss).

Statistical analysis

Statistical analysis was performed using analysis of variance test.

RESULTS

The rS1/9 scaffolds: Structure, mechanical properties, and degradation

Scaffolds were prepared by salt leaching method from purified rS1/9 protein, a recombinant analogue of spidroin 1 from *N. clavipes*. The structure of scaffolds was examined using SEM or CLSM in aqueous environment. Figure 1(A) shows a SEM cross-section of the scaffold. The macropores of scaffolds are interconnected via channels and openings. Additionally, the aggregated rS1/9 molecules spontaneously formed a sponge-like microporous structure of the walls of macropores [Fig. 1(B,C)]. The micropores were also interconnected and formed a network because of openings on the surface of walls. The micropores were 2–10 μm in diameter.

Mechanical tests were conducted to estimate the tensile strength and extensibility of the bar-shaped porous scaffolds. The tensile strength of scaffolds was 18 ± 5 N/cm^2, and the extensibility was >50%. Studies of scaffold degradation showed that the scaffolds were quite stable in PBS but degradable by oxidation in Fenton's reagent by 11th week ($p < 0.05$ between weeks 1 and 11; Fig. 2).

Cell adhesion and growth on the rS1/9 films

The ability of the rS1/9 biopolymer to support cell adhesion and proliferation in a culture on the surface of the rS1/9 films was studied. Average number of fibroblasts per 1 mm^2 of the film and total amount of grown cells are shown in Figure 3. The total cell number increased both on biopolymer films and glass surface (control) for up to 4 days ($p <$

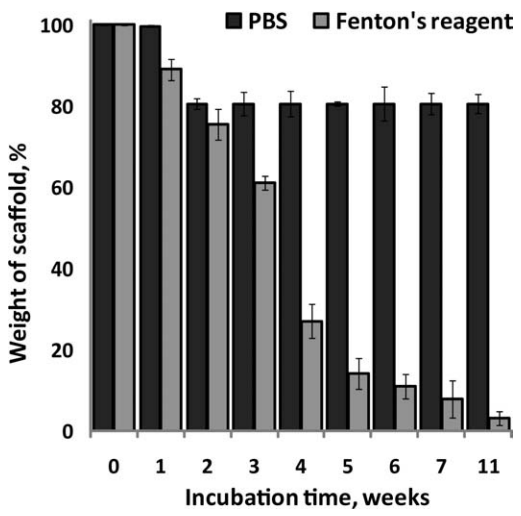

FIGURE 2. Degradation of the rS1/9 scaffolds in PBS and in Fenton's reagent. The scaffolds were stable in PBS but were destroyed in Fenton's reagent. The data are mean ± standard deviation of three independent measurements. Significant differences were detected between PBS and Fenton's reagent groups after week 2 of incubation ($p < 0.05$).

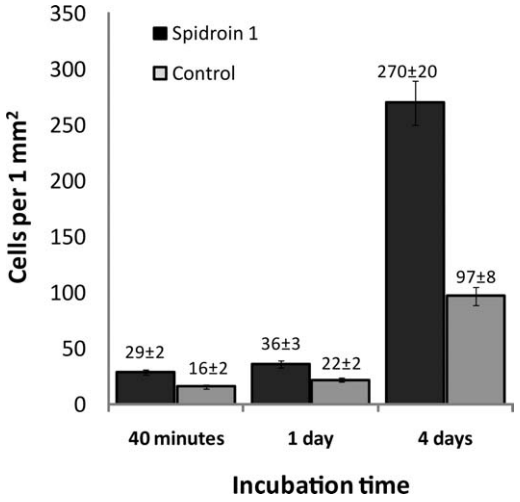

FIGURE 3. Culture of 3T3 fibroblasts on the rS1/9 films. CLSM images were used for quantification. The data are mean ± standard deviation of five independent measurements. Significant difference was detected between the quantities of cells on the glass surface *versus* the film and between the first and the last time points for both glass and film surfaces ($p < 0.01$).

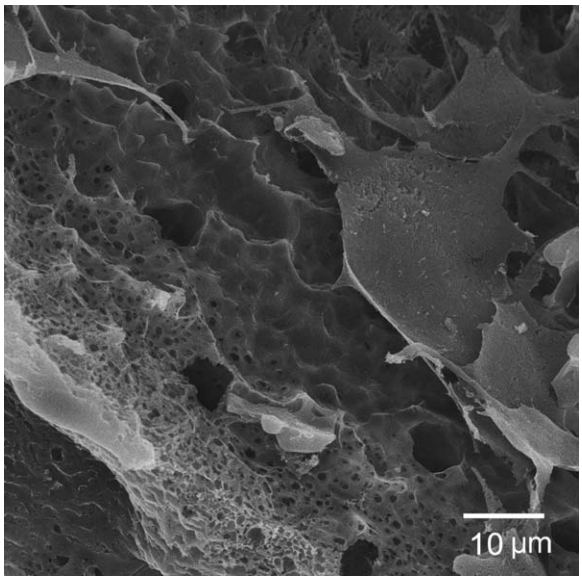

FIGURE 4. SEM image of 3T3 fibroblasts on the surface of macropores of the rS1/9 scaffold. Cells were grown on the scaffold for 9 days. Scaffolds were processed for SEM and cut. The view shown is from the inner side of the scaffold (300 μm from the surface). Note the spread morphology of cells on the surface of scaffolds. Openings of the micropores are visible.

0.01 between "day 0" and "day 4" groups). Importantly, the number of cells grown on the rS1/9 films was greater than that on the glass ($p < 0.01$).

Next, the ability of the rS1/9 scaffolds to maintain cell adhesion and proliferation was tested. Typical spread morphology of 3T3 fibroblasts on the microporous surface of the rS1/9 scaffolds was observed (Fig. 4). Average number of cells per mm^3 of each sample was determined using stacked CLSM images that allow for a noninvasive observation of cells inside the scaffold [Fig. 5(A)]. Proliferation of 3T3 fibroblasts was determined by calculating the number of cells in scaffolds after 1, 3, and 14 days. The increase in the number of cells [$p < 0.01$; Fig. 5(B)] during incubation with scaffolds was observed. After 2 weeks, cell distribution inside the scaffold changed gradually from a nonuniform ($p < 0.05$ between the layers) to uniform ($p > 0.05$) pattern. The rate of proliferation varied with the depth of the rS1/9 scaffold. The number of cells increased 11-fold at depth more than 300 μm and only 2.5-fold with depth up to 150 μm (Table I).

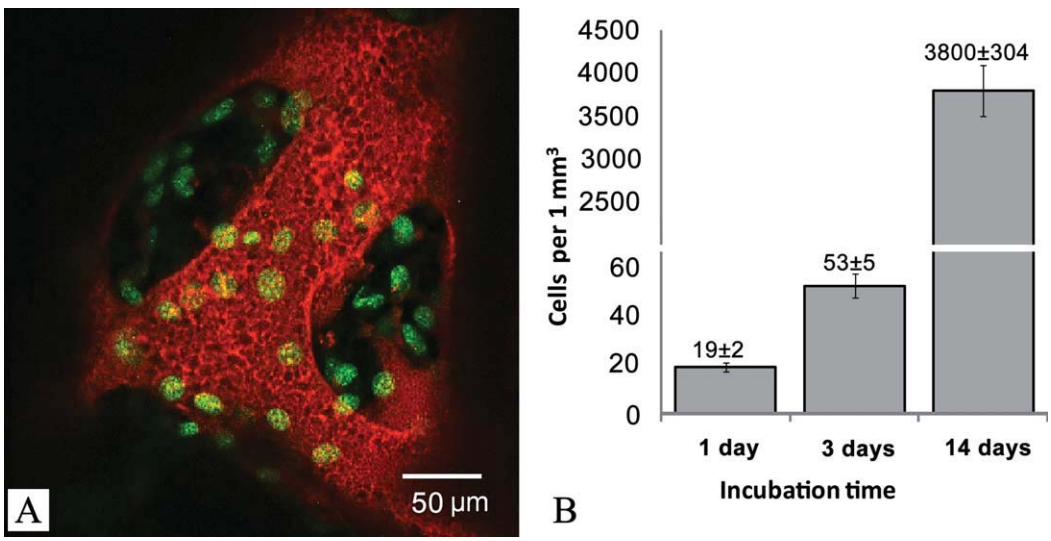

FIGURE 5. Culture of 3T3 cells inside the rS1/9 scaffolds. (A) CLSM images were used for cell quantitation. Nuclei were visualized with SYTOX Green. Microstructure of the scaffolds was visualized using tetramethyl rhodamine iso-thiocyanate. (B) Increase of cell number within the scaffold. The data are mean ± standard deviation for five measurements. Statistically significant differences were found between 3-day and 14-day groups *versus* 1-day group as well as between days 14 and 3 ($p < 0.01$). [Color figure can be viewed in the online issue, which is available at wileyonlinelibrary.com.]

In vivo biocompatibility of the rS1/9 scaffolds

The rS1/9 scaffolds implanted subcutaneously in BALB/c mice caused no serious pathological signs. After 8 weeks, the scaffolds were incompletely enveloped by thin vascularized tissue. A significant tissue ingrowth was observed: the macropores of scaffolds were infiltrated with the host fibrous and adipose tissue elements (Fig. 6). Cells of invaded tissue were tightly attached to the surface of the implant, demonstrating good adhesive properties of scaffold surface *in vivo* [Fig. 5(A,B)]. Scaffolds were infiltrated with macrophages and single multinuclear giant cells, comprising a foreign-body-type reaction [Fig. 6(B)]. The rS1/9 scaffolds lost their structural integrity, and the walls of macropores were perforated [Fig. 6(A)]. A significant vascularization in implanted scaffolds was observed [Fig. 6(B)]. Furthermore, an ingrowth of nerve fibers was detected in the implanted scaffolds [Fig. 6(B,C)]. Dense connective tissue formed a sheath around the nerve fibers. Inside the connective tissue, the axon bundles were grouped together to form nerve fascicles. The axis cylinders of some nerve fibers were enclosed within myelin sheath. The nuclei of glial cells were visualized around myelinated and nonmyelinated nerve fibers [Fig. 6(C)].

DISCUSSION

Spider silk is an attractive material for tissue engineering because it possesses a unique combination of physicochemical properties such as elasticity and toughness, biodegradability, and resistance to environmental cues.[15] The biopolymer rS1/9 reproduces conformational characteristics and properties of natural analogue, including ability to form submolecular forms and aggregates (nanofibrils, films, capsules, and threads). There is an inverse correlation of recombinant protein length and its yield; nevertheless, relatively long-length analogues of a protein can be effectively produced in bacterial or yeasts cells.[16] The main advantage of recombinant proteins is the possibility to modify the structure by inserting an additional amino acid sequence for high cell - adhesion (RGD) or biologically active molecules.[17,18] The rS1/9 biopolymer has promising physical and chemical properties and may be used for preparation of fibrils and thin films.[12,13] Here, the salt leaching technique was applied to form rS1/9 scaffolds. The prepared scaffolds have interconnected macroporous structures [Fig. 1(A)], a prerequisite for a cell culture. In addition to macropores, the scaffolds also have a spontaneously formed microporous structure [Fig. 1(B,C)] that enhances the interconnectivity. The rS1/9 biopolymer has been shown to spontaneously adopt a

TABLE I. Distribution of 3T3 Cells Within rS1/9 Scaffolds

Scaffold Layer (Depth, μm)	Number of Cells (%)	
	1 Day	2 Weeks
0–150	58 ± 7	27 ± 8
150–300	31 ± 3[a]	40 ± 4
300–450	11 ± 8[a]	33 ± 4

[a] $p < 0.05$ compared with 0–150 μm layer. $N = 3$.

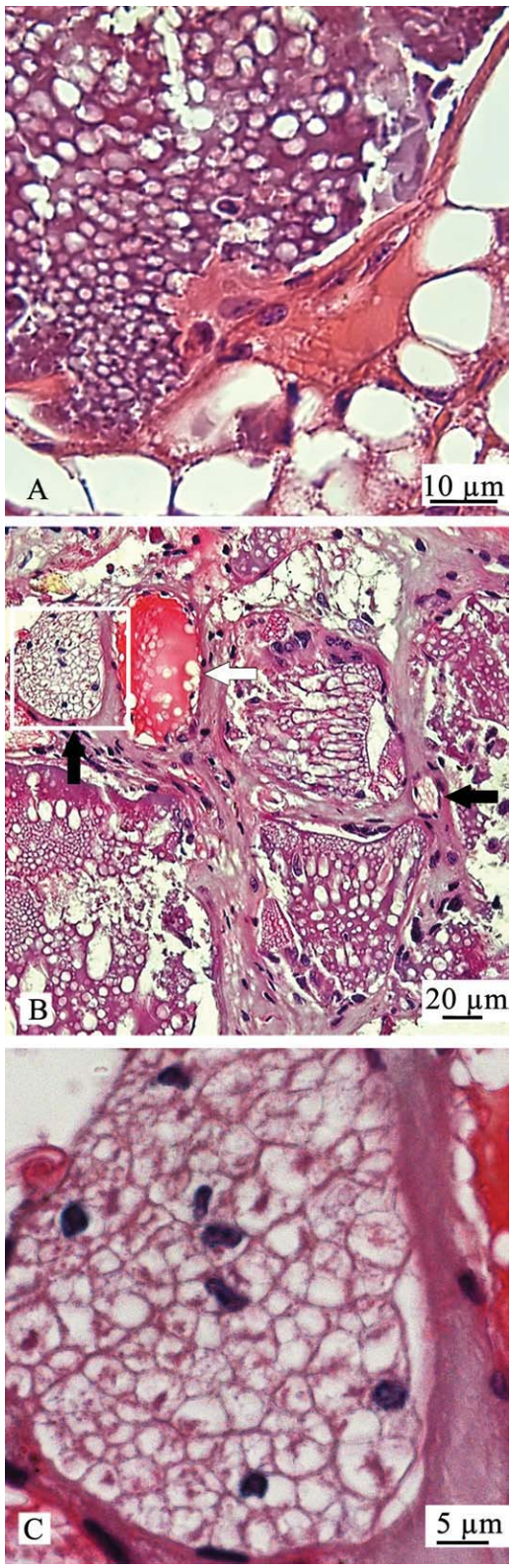

FIGURE 6. Hematoxylin and eosin staining of histological sections of the rS1/9 scaffolds. Scaffolds were implanted subcutaneously in BALB/c mice for 8 weeks. (A) Penetration of connective tissue cells into the scaffold. (B) Ingrowth of vascularized tissue with nerve fibers. White arrow denotes a vessel, black arrows denote nerve fibers. (C) Magnified image of a nerve fiber (shown in a square in B).

similar structure in films.[13] The spontaneously formed scaffold microstructure described in this study has not been reported so far. The micropore-like structure of rS1/9 scaffolds and films might be a specific feature of rS1/9 protein. Natural spider fibrils do not seem to possess microporous structure,[16] and the shorter analogues of spidroin (e.g., small-length analogues of silk of spiders *Euprosthenops australis*[19] and *Araneus diadematus*[20]) do not form microporous structure on aggregation.

Mechanical properties of silk biopolymers are associated with a structural transition from nonorganized loops to beta-sheet conformations. Treatment of the rS1/9 biopolymer with ethanol, a procedure used in preparation of scaffolds, promotes this structural transition.[21] However, unlike natural spider silk, rS1/9 protein is small (molecular weight is ~94 kDa). Despite the fact that rS1/9 protein is capable of spontaneous conformational transition to a highly crystalline structure,[13] the structure should be weaker because of a small size of the rS1/9. The tensile strength of scaffolds is lower than that of the rS1/9 fibers, supposedly because of a noncompact, ruptured surface prone to cracking. Other authors have also shown that currently available recombinant spidroin 1 are less strong than natural polymer fibers.[13,22,23]

The structure of the rS1/9 scaffold, being stable in PBS, can be rapidly destroyed *in vitro* by oxidizing Fenton's reagent (Fig. 2). Such model mimics the conditions observable in an acute tissue response.[24] One may hypothesize that the sensitivity to oxidation might be beneficial for biodegradation at the sites of implantation because the scaffolds could be replaced by host tissues.

The characteristics of the polymer-formed substrate and the structure of the surface are crucial for cell adhesion and proliferation. Some natural spider silks have been successfully used as a substrate material for cell culture,[19,25,26] whereas, in some reports, the spider silks evoked unfavorable effects on eukaryotic cells.[17,27] Data on *in vitro* biocompatibility of natural silk of *N. clavipes* is limited; however, several modified recombinant spidroin 1 proteins demonstrated good biocompatibility.[28–30] The rS1/9 biopolymer supported cell adhesion and proliferation, as determined by a higher adhesiveness of the rS1/9 compared with glass support (Fig. 3). Moreover, the number of cells on the surface of the rS1/9 films increased with a higher rate than in control. Thus, the substrate properties of the rS1/9 make this biopolymer suitable for eukaryotic cell culture.

The macroporous and microporous interconnected structure of scaffolds is a prerequisite for a long-term cell culture. An interconnected structure enables cells to migrate deeply inside the scaffold; furthermore, such structure allows for gas exchange, effective nutrient supply, and metabolic waste removal. Furthermore, the microstructure of the scaffolds contributes to cell adhesion.[1,31–35] Scaffolds with a generated microporous structure have been used for cell culture.[31,36,37] The surface openings of the micropores and their diameter can also influence the adhesion and growth of cells.[35,38] Typical spread morphology of fibroblasts inside the scaffold was observed (Figs. 4 and 5). The time course of cell distribution revealed that the cells could migrate inside the scaffold (Table I). These data strongly suggest that the complex structure of the rS1/9 scaffolds forms an environment suitable for cell culture.

Until now, investigations of postimplantation biocompatibility of spider silks in tissue engineering have been limited to natural spider silk of *A. diadematus*[25] and a recombinant analogue of silk of *E. australis*.[39] Natural silk of *Nephila* spider was used for guiding nerve growth *in vivo*.[40] The scaffolds of macroporous and microporous structure were well tolerated by animals for at least 60 days. A significant tissue ingrowth and the replacement of scaffold material with newly formed tissue (Fig. 6) were detected. The interconnected structure of the scaffold promoted homogeneous tissue ingrowth. The observed infiltration of the implanted scaffold with macrophages and giant cells is a typical foreign body response. This reaction was mild and comparable with the reported tissue reaction to silk implants.[39,41,42]

Accumulation of macrophages and their functional activities are modulated by the microporous structure of the implant[9,43] and the diameter of the openings of the micropores. Macrophages play a critical role in silk scaffold degradation, promoting the replacement of scaffold with the host tissue. The material properties such as the structure, the microporous texture of the surface, and the accumulation of macrophages[9,43,44] could contribute to the ability of the implants to support angiogenesis. A significant vascularization of the rS1/9 scaffold (Fig. 6) proves that the conditions for *de novo* vessel formation were favorable. Finally, the ingrowth of nerve fibers into implanted scaffolds demonstrated in this study seems to be an interesting and a rarely reported event. This phenomenon can be related to the accumulation of macrophages[45] and angiogenesis inside the implanted scaffolds.[46]

CONCLUSIONS

The rS1/9 scaffolds possess a unique microporous structure of the walls of macropores. Scaffolds are stable in PBS and can degrade in oxidizing environment with weight decreasing up to 90% after week 11 of incubation. The rS1/9 scaffolds show good biocompatible properties *in vitro* and *in vivo*. After implantation, scaffolds promote ingrowth of fibrous, nerve, and adipose tissue elements, as well as angiogenesis. The rS1/9 scaffolds can be applicable in biomedical tissue engineering.

ACKNOWLEDGMENTS

The authors are grateful to E. Pechnikova for the excellent assistance in SEM imaging.

REFERENCES

1. Bacakova L, Filova E, Rypacek F, Svorcik V, Stary V. Cell adhesion on artificial materials for tissue engineering. Physiol Res 2004; 53(Suppl 1):S35–S45.
2. Lee J, Cuddihy MJ, Kotov NA. Three-dimensional cell culture matrices: State of the art. Tissue Eng Part B Rev 2008;14:61–86.
3. Sevastianov VI, Vasilets VN, Agapov II. Biopolymer implants for high-technology assistance in the field of replacement and regenerative medicine. Rare Metals 2009;28:84–86.

4. Altman GH, Diaz F, Jakuba C, Calabro T, Horan RL, Chen J, Lu H, Richmond J, Kaplan DL. Silk-based biomaterials. Biomaterials 2003;24:401–416.
5. Acharya C, Ghosh SK, Kundu SC. Silk fibroin protein from mulberry and non-mulberry silkworms: Cytotoxicity, biocompatibility and kinetics of L929 murine fibroblast adhesion. J Mater Sci Mater Med 2008;19:2827–2836.
6. Asakura T, Tanaka C, Yang M, Yao J, Kurokawa M. Production and characterization of a silk-like hybrid protein, based on the polyalanine region of *Samia cynthia ricini* silk fibroin and a cell adhesive region derived from fibronectin. Biomaterials 2004;25: 617–624.
7. Gosline JM, Guerette PA, Ortlepp CS, Savage KN. The mechanical design of spider silks: From fibroin sequence to mechanical function. J Exp Biol 1999;202:3295–3303.
8. Li M, Tao W, Lu S, Zhao C. Porous 3-D scaffolds from regenerated *Antheraea pernyi* silk fibroin. Polym Adv Technol 2008;19: 207–212.
9. Campbell CE, von Recum AF. Microtopography and soft tissue response. J Invest Surg 1989;2:51–74.
10. Arcidiacono S, Mello C, Kaplan D, Cheley S, Bayley H. Purification and characterization of recombinant spider silk expressed in *Escherichia coli*. Appl Microbiol Biotechnol 1998;49:31–38.
11. Scheller J, Guhrs KH, Grosse F, Conrad U. Production of spider silk proteins in tobacco and potato. Nat Biotechnol 2001;19: 573–577.
12. Bogush VG, Sazykin AY, Davydova LI, Martirosyan VV, Sidoruk KV, Glazunov AV, Akishina RI, Shmatchenko NA, Debabov VG. Obtaining, purification and silking of recombinant analog of spidroin 1. Biotechnology (Mosc) 2006;4:1–15.
13. Bogush VG, Sokolova OS, Davydova LI, Klinov DV, Sidoruk KV, Esipova NG, Neretina TV, Orchanskyi IA, Makeev VY, Tumanyan VG, Shaitan KV, Debabov VG, Kirpichnikov MP. A novel model system for design of biomaterials based on recombinant analogs of spider silk proteins. J Neuroimmune Pharmacol 2009;4:17–27.
14. Fahnestock SR, Yao Z, Bedzyk LA. Microbial production of spider silk proteins. J Biotechnol 2000;74:105–119.
15. Kluge JA, Rabotyagova O, Leisk GG, Kaplan DL. Spider silks and their applications. Trends Biotechnol 2008;26:244–251.
16. Teule F, Cooper AR, Furin WA, Bittencourt D, Rech EL, Brooks A, Lewis RV. A protocol for the production of recombinant spider silk-like proteins for artificial fiber spinning. Nat Protoc 2009;4: 341–355.
17. Huang J, Wong C, George A, Kaplan DL. The effect of genetically engineered spider silk-dentin matrix protein 1 chimeric protein on hydroxyapatite nucleation. Biomaterials 2007;28:2358–2367.
18. Wong Po FC, Patwardhan SV, Belton DJ, Kitchel B, Anastasiades D, Huang J, Naik RR, Perry CC, Kaplan DL. Novel nanocomposites from spider silk-silica fusion (chimeric) proteins. Proc Natl Acad Sci U S A. 2006;103:9428–9433.
19. Stark M, Grip S, Rising A, Hedhammar M, Engstrom W, Hjalm G, Johansson J. Macroscopic fibers self-assembled from recombinant miniature spider silk proteins. Biomacromolecules 2007;8: 1695–1701.
20. Lazaris A, Arcidiacono S, Huang Y, Zhou JF, Duguay F, Chretien N, Welsh EA, Soares JW, Karatzas CN. Spider silk fibers spun from soluble recombinant silk produced in mammalian cells. Science 2002;295:472–476.
21. Chen X, Shao Z, Marinkovic NS, Miller LM, Zhou P, Chance MR. Conformation transition kinetics of regenerated *Bombyx mori* silk fibroin membrane monitored by time-resolved FTIR spectroscopy. Biophys Chem 2001;89:25–34.
22. Fahnestock SR. Novel, recombinantly produced spider silk analogs. Int. Application #PCT/US94/06689. Int. Publication #WO 94/ 29450. 1994.
23. Seidel A, Liivak O, Calve S, Adaska J, Ji G, Yang Z, Grubb D, Zax DB, Jelinski LW. Regenerated spider silk: Processing, properties, and structure. Macromolecules 2009;33:775–780.
24. Winyard PG, Perret D, Harris G, Blake DR. The role of toxic oxygen species in inflammation with special reference to DNA damage. In: Whitcher J, Evans S, editors. Biochemistry of Inflammation. Lancaster: Kluwer Academic Publishers; 2009. p 112.
25. Gellynck K, Verdonk P, Forsyth R, Almqvist KF, Van NE, Gheysens T, Mertens J, Van LL, Kiekens P, Verbruggen G. Biocompatibility and biodegradability of spider egg sac silk. J Mater Sci Mater Med 2008;19:2963–2970.
26. MacIntosh AC, Kearns VR, Crawford A, Hatton PV. Skeletal tissue engineering using silk biomaterials. J Tissue Eng Regen Med 2008;2:71–80.
27. Hakimi O, Gheysens T, Vollrath F, Grahn MF, Knight DP, Vadgama P. Modulation of cell growth on exposure to silkworm and spider silk fibers. J Biomed Mater Res A 2009;92:1366–1372.
28. Bini E, Foo CW, Huang J, Karageorgiou V, Kitchel B, Kaplan DL. RGD-functionalized bioengineered spider dragline silk biomaterial. Biomacromolecules 2006;7:3139–3145.
29. Morgan AW, Roskov KE, Lin-Gibson S, Kaplan DL, Becker ML, Simon CG Jr. Characterization and optimization of RGD-containing silk blends to support osteoblastic differentiation. Biomaterials 2008;29:2556–2563.
30. Scheller J, Henggeler D, Viviani A, Conrad U. Purification of spider silk-elastin from transgenic plants and application for human chondrocyte proliferation. Transgen Res 2004;13:51–57.
31. Cai Q, Yang J, Bei J, Wang S. A novel porous cells scaffold made of polylactide-dextran blend by combining phase-separation and particle-leaching techniques. Biomaterials 2002;23:4483–4492.
32. Lampin M, Warocquier C, Legris C, Degrange M, Sigot-Luizard MF. Correlation between substratum roughness and wettability, cell adhesion, and cell migration. J Biomed Mater Res 1997;36: 99–108.
33. Mata A, Su X, Fleischman AJ, Roy S, Banks BA, Miller SK, Midura RJ. Osteoblast attachment to a textured surface in the absence of exogenous adhesion proteins. IEEE Trans Nanobiosci 2003;2:287–294.
34. Singhvi R, Stephanopoulos G, Wang DI. Effects of substratum morphology on cell physiology. Biotechnol Bioeng 1994;43:764–771.
35. Von Recum AF, Shannon CE, Cannon CE, Long KJ, Van Kooten TG, Meyle J. Surface roughness, porosity, and texture as modifiers of cellular adhesion. Tissue Eng 1996;2:241–253.
36. Gao J, Crapo PM, Wang Y. Macroporous elastomeric scaffolds with extensive micropores for soft tissue engineering. Tissue Eng 2006;12:917–925.
37. Ilagan BG, Amsden BG. Macroporous photocrosslinked elastomer scaffolds containing microporosity: Preparation and in vitro degradation properties. J Biomed Mater Res A 2010;93:211–218.
38. Lee JH, Lee SJ, Khang G, Lee HB. Interaction of fibroblasts on polycarbonate membrane surfaces with different micropore sizes and hydrophilicity. J Biomater Sci Polym Ed 1999;10:283–294.
39. Fredriksson C, Hedhammar M, Feinstein R, Nordling K, Kratz G, Johansson J, Huss F, Rising A. Tissue response to subcutaneously implanted recombinant spider silk: An in vivo study. Materials 2009;2:1908–1922.
40. Allmeling C, Jokuszies A, Reimers K, Kall S, Choi CY, Brandes G, Kasper C, Scheper T, Guggenheim M, Vogt PM. Spider silk fibres in artificial nerve constructs promote peripheral nerve regeneration. Cell Prolif 2008;41:408–420.
41. Meinel L, Hofmann S, Karageorgiou V, Kirker-Head C, McCool J, Gronowicz G, Zichner L, Langer R, Vunjak-Novakovic G, Kaplan DL. The inflammatory responses to silk films in vitro and in vivo. Biomaterials 2005;26:147–155.
42. Wang Y, Rudym DD, Walsh A, Abrahamsen L, Kim HJ, Kim HS, Kirker-Head C, Kaplan DL. In vivo degradation of three-dimensional silk fibroin scaffolds. Biomaterials 2008;29:3415–3428.
43. Padera RF, Colton CK. Time course of membrane microarchitecture-driven neovascularization. Biomaterials 1996;17:277–284.
44. Brauker JH, Carr-Brendel VE, Martinson LA, Crudele J, Johnston WD, Johnson RC. Neovascularization of synthetic membranes directed by membrane microarchitecture. J Biomed Mater Res 1995;29:1517–1524.
45. Miyauchi A, Kanje M, Danielsen N, Dahlin LB. Role of macrophages in the stimulation and regeneration of sensory nerves by transposed granulation tissue and temporal aspects of the response. Scand J Plast Reconstr Surg Hand Surg 1997;31:17–23.
46. Gibran NS, Tamura R, Tsou R, Isik FF. Human dermal microvascular endothelial cells produce nerve growth factor: Implications for wound repair. Shock 2003;19:127–130.